

Adrenergic signalling between rat taste receptor cells

Scott Herness *†, Fang-li Zhao *, Namik Kaya *, Shao-gang Lu *, Tiansheng Shen * and Xiao-Dong Sun ‡

*Department of Oral Biology, College of Dentistry, Ohio State University, 305 West 12th Avenue, Columbus, OH 43210, †Department of Neuroscience, College of Medicine, Ohio State University, 333 West 10th Avenue, Columbus, OH 43210 and ‡Preclinical Toxicology Infectious Disease/Safety Pharmacology, Pharmacia Corporation, 7270-300-130, 301 Henrietta Street, Kalamazoo, MI 49007, USA

In taste buds, synaptic transmission is traditionally thought to occur from taste receptor cells to the afferent nerve. This communication reports the novel observation that taste receptor cells respond to adrenergic stimulation. Noradrenaline application inhibited outward potassium currents in a dose-dependent manner. This inhibition was mimicked by the β agonist isoproterenol and blocked by the β antagonist propranolol. The α agonists clonidine and phenylephrine both inhibited the potassium currents and elevated intracellular calcium levels. Inwardly rectifying potassium currents were unaffected by adrenergic stimulation. Experiments using the RT-PCR technique demonstrate that lingual epithelium expresses multiple α ($\alpha 1a$, $\alpha 1b$, $\alpha 1c$, $\alpha 1d$, $\alpha 2a$, $\alpha 2b$, $\alpha 2c$) and β ($\beta 1$, $\beta 2$) subtypes of adrenergic receptors, and immunocytochemistry localized noradrenaline to a subset of taste receptor cells. Collectively, these data imply strongly that adrenergic transmission within the taste bud may play a paracrine role in taste physiology.

(Received 5 April 2002; accepted after revision 26 June 2002)

Corresponding author M. S. Herness: College of Dentistry, Ohio State University, 305 West 12th Avenue, P.O. Box 182357, Columbus, OH 43218-2357, USA. Email: herness.1@osu.edu

In vertebrates, the peripheral portion of the gustatory system is composed of two cell types, a taste receptor cell and an afferent neurone. Taste receptor cells, which are differentiated epithelial cells, are sequestered into specialized structures referred to as taste buds; some of the cells within the bud are synaptically connected to the afferent nerve. Although synaptic structures between taste cell types and nerve fibres have been characterized at an ultrastructural level (e.g. Finger & Simon, 2000), the transmitter that operates within the taste bud is not known with certainty. Accumulating evidence suggests that multiple transmitters may be operative in rodent taste buds (reviewed in Nagai *et al.* 1996; Yamamoto *et al.* 1998). In rat taste buds, evidence exists for at least five transmitters, namely serotonin, glutamate, GABA, noradrenaline and acetylcholine, each with varying levels of supportive data.

Of these putative candidates, serotonin and glutamate have been the best studied at both physiological and molecular levels of analysis. Evidence for serotonin and serotonin transporter in rodent taste receptor cells has been demonstrated immunocytochemically (Kim & Roper, 1995; Ren *et al.* 1999). The physiological responses of rat taste receptor cells to serotonin have also been demonstrated electrophysiologically. Inhibition of a calcium-activated potassium current and, at higher serotonin concentrations, a voltage-dependent sodium current, have been recorded with whole-cell patch-clamp recordings (Herness & Chen, 1997, 2000). Pharmacological evidence suggests that these effects are mediated by 5HT-1A

receptors. These reports were significant for another reason in that they provided support for the notion of cell-to-cell communication in rodent taste buds by demonstrating that taste receptor cells, in addition to afferent nerves, respond to neurotransmitter.

Unlike serotonin, the role of glutamate in rodent taste buds is more complicated since it serves as both a neurotransmitter and a taste stimulus (referred to as umami). It is likely that several types of glutamate receptors are present in rodent taste buds, including metabotropic receptors, ionotropic receptors, a novel truncated variant of mGluR4 (Chaudhari & Roper *et al.* 1996, 2000) that likely serves as the umami receptor, and a dimer of the T1R family (T1R1+3) that serves as an amino-acid receptor (Nelson *et al.* 2002). Physiological and pharmacological evidence suggests that rat taste receptor cells respond to stimulation of these receptors in manners appropriate for tastant or transmitter actions (Bigiani *et al.* 1997; Lin & Kinnamon, 1999). Evidence in support of a role for glutamate as a neurotransmitter in rat taste buds includes glutamate-stimulated cobalt uptake (Caicedo *et al.* 2000b) and calcium imaging (Caicedo *et al.* 2000a). These responses were localized to basolateral portions of the cells with a concentration–response function consistent with glutamate as a transmitter rather than as a tastant.

Less evidence exists for the remaining three candidates. GABA and a GABA transporter, GAT3, have been localized to subsets of taste receptor cells in rats with immunocytochemical techniques (Obata *et al.* 1997),

although no physiological data yet exists to delineate a functional role for GABA in the taste bud. Acetylcholine, on the other hand, causes large increases in intracellular calcium in rat posterior taste cells via muscarinic receptors (personal observations), but studies to localize acetylcholine to taste receptor cells are not extant.

This communication concerns adrenergic stimulation. In parallel with studies on serotonin, taste receptor cells have been demonstrated to respond to the neurotransmitter noradrenaline. Exogenous noradrenaline enhances a calcium-activated chloride current via β -adrenergic receptors (Herness & Sun, 1999). In this communication, evidence is presented that noradrenaline acts to inhibit an outward potassium current as well as to elevate intracellular calcium. Pharmacological studies and RT-PCR experiments suggest the involvement of both α and β receptors. Moreover, immunocytochemistry suggests that taste receptor cells are the endogenous source of noradrenaline within the taste bud. Collectively, these data may serve as the basis for discussion of a putative paracrine role of adrenergic transmission in peripheral gustatory physiology.

METHODS

Dissociation procedure

Patch-clamp and calcium-imaging experiments were performed on taste receptor cells isolated from the circumvallate and foliate papillae of Sprague-Dawley rats as described previously (e.g. Herness & Sun, 1995). All procedures were approved by the University's Laboratory Animal Care and Use Committee and adhered to the NIH 'Guide for the Care and Use of Laboratory Animals'. Animals were anaesthetized with an intramuscular injection of 0.09 ml 100 (g body weight)⁻¹ ketamine-acepromazine mixture (91 mg ml⁻¹ ketamine, Fort Dodge Laboratories; 0.09 mg ml⁻¹ acepromazine, Butler Laboratories). While under a surgical level of anaesthesia, animals were decapitated and lingual tissue was excised. The divalent-free solution for enzymatic incubation was composed of (mM): 80 NaCl, 5 KCl, 26 NaHCO₃, 2.5 NaH₂PO₄·1H₂O, 20 D-glucose and 1 EDTA to which cysteine-activated (1 mg ml⁻¹) papain (14 U ml⁻¹) was added. The standard extracellular fluid (ECF) comprised (mM): 126 NaCl, 1.25 NaH₂PO₄·1H₂O, 5 KCl, 5 NaHepes, 2 MgCl₂, 2 CaCl₂ and 10 glucose, to pH 7.4 with NaOH. The pseudo-intracellular fluid (ICF) used for filling the recording pipette comprised (mM): 140 KCl, 2 MgCl₂, 1 CaCl₂, 11 EGTA, 10 Hepes and 4 ATP (disodium salt).

Whole-cell electrophysiological recording

The micropipettes used for whole cell recording were pulled from 1.5 mm o.d. borosilicate glass (World Precision Instruments, Sarasota, FL, USA) with typical resistances of 4–7 M Ω . Junction potentials were corrected; seal resistances were typically several decades of gigaohms. For amphotericin-B perforated-patch recordings (400 g ml⁻¹), approximately 30 min was required to reach a stable level of recording after gigaseal formation. Fast and slow capacitance compensation was employed as necessary with amplifier controls. Cell membrane capacitance and uncompensated series resistance were adjusted to produce optimal transient balancing. Membrane capacitance was 3–6 pF; series

resistance averaged 10 M Ω in conventional whole-cell mode and 20–50 M Ω in most amphotericin-B perforated patch-clamp recordings.

Data were acquired with a high-impedance amplifier (Axopatch 200-B; Axon Instruments), a Pentium-based 450 MHz computer, a 12 bit 330 kHz A/D converter (Digidata 1200; Axon Instruments) and a commercial software program (pCLAMP, versions 7.0 or 8.01; Axon Instruments). Membrane currents were acquired after low-pass filtering with a cut-off frequency of 10 kHz (at -3 dB). A software-driven D/A converter generated the voltage protocols. In most situations, currents were measured with voltage protocols using command step potentials of 80 ms duration from a holding potential of -80 mV applied in 10 mV increments to a final potential of +90 mV. A P/4 leak subtraction protocol was employed. For recording inwardly rectifying potassium currents (K_{IR}), the membrane voltage was typically held at its zero-current potential (in 100 mM extracellular potassium), usually around -3 to -10 mV, and a series of depolarizing or hyperpolarizing command potentials, in 10 mV increments, was applied ranging from -160 mV to +30 mV (Sun & Herness, 1996). Leak subtraction was not employed for the study of K_{IR}.

Data were analysed with a combination of off-line software programs that included a software acquisition suite (pCLAMP, Axon Instruments) and a technical graphics/analysis program (Origin 6.0; MicroCal Software). Exchange of the bathing solution was accomplished with a gravity-fed perfusion system at approximately 2 ml min⁻¹. Several minutes were allowed for exchange of bath volume, which was estimated to be 0.9 ml. Data were normalized to the value of the current magnitude before drug application. Pooled Student's one-tailed *t* test was used to evaluate statistical difference between means, considered significant at values of *P* < 0.05, although values were typically < 0.001. Data are presented as means \pm S.E.M.

Calcium imaging

Intracellular calcium levels in dissociated taste receptor cells were monitored using standard ratiometric techniques. Images were acquired with a CCD camera (Hamamatsu Orka, Hamamatsu Photonic KK, Hamamatsu City, Japan) through an oil-immersion $\times 40$ objective lens on an inverted microscope driven by commercially available software (SimplePCI, Compix, Cranberry Twp, PA, USA). Cells were loaded with fura-2 AM ester (5 μ M, dissolved in DMSO) in the presence of a dispersing reagent, 0.05% Pluronic F-127 (dissolved in DMSO) and 1% bovine serum albumin for 60 min, then washed with normal ECF for at least 20 min. Pairs of fluorescent images were recorded at 340 or 380 nm excitation. Excitation wavelengths were produced with a software-driven monochromator (Polychrome II, Photonics, Applied Scientific Instrumentation, Eugene, OR, USA). Light was collected through a 510 nm emission filter. Paired images were obtained once every 6 s during the stimulation period and every 1–2 min during baseline measurements.

Stimuli were applied with a perfusion system that allowed focal application of one of eight stimuli, controlled by Teflon valves, channelled into a quartz pipette that was positioned close to the cell with a micromanipulator (ValueLink 8, Automate Scientific, Oakland, CA, USA). Stimuli were presented against a slow background perfusion of ECF and allowed quick focal application or removal of the stimulus (< 1 s). Ratios (340/380) before, during and after stimulus presentation were taken to reflect changes of intracellular calcium in response to the stimulus.

Table 1. Primer sequences used in RT-PCR reactions for adrenergic receptor subtypes

Target	Primers 5'-Sense-3'; 5'-Antisense-3'	Expected product size	Reference
$\alpha 1a$	GTA GCC AAG AGA GAA AGC CG CAA CCC ACC ACG ATG CCC AG	212 bp	Scotfield <i>et al.</i> 1995
$\alpha 1b$	GCT CCT TCT ACA TCC CGC TCG AGG GGA GCC AAC ATA AGA TGA	300 bp	Scotfield <i>et al.</i> 1995
$\alpha 1c$	TGG CCA TCA TTC TGG TTA TGT GCA ACC CAC CAC GAT GCC CAG	251 bp	Gould <i>et al.</i> 1995
$\alpha 1d$	CGT GTG CTC CTT CTA CCT ACC GCA CAG GAC GAA GAC ACC CAC	304 bp	Scotfield <i>et al.</i> 1995
$\alpha 2a$	GCG CCC CAG AAC CTC TTC CTG GTG CCA GCG CCC TTC TTC TCT ATG GAG	312 bp	Vidovic <i>et al.</i> 1994
$\alpha 2b$	AAA CGC AGC CAC TGC AGA GGT CTC ACT GGC AAC TCC CAC ATT CTT GCC	456 bp	Vidovic <i>et al.</i> 1994
$\alpha 2c$	CTG GCA GCC GTG GTG GGT TTC CTC GTC GGG CCG GCG GTA GAA AGA GAC	425 bp	Vidovic <i>et al.</i> 1994
$\beta 1$	CGC TCA CCA ACC TCT TCA TCA TGT CC CAG CAC TTG GGG TCG TTG TAG GAG C	376 bp	Troispoux <i>et al.</i> 1998
$\beta 2$	TCT TCG AAA ACC TAT GGG AAC GGC GGA TGT GCC CCT TCT GCA AAA TCT	343 bp	Troispoux <i>et al.</i> 1998
$\beta 3$	GCT ATG CCA ACT CTG CCT TCA ACC GCG GCT GAG GTA GTA GCG AAG TTC AA	478 bp	Troispoux <i>et al.</i> 1998
Gustducin	GTT GGC TGA AAT AAT TAA ACG ATC TCT GGC CAC CTA CAT C	231 bp	McLaughlin <i>et al.</i> 1992
GAPDH	GAT GCT GGT GCT GAG TAT GTC G GTG GTG CAG GAT GCA TTG CTC TGA	200 bp	Fort <i>et al.</i> 1985, Zhao <i>et al.</i> 1995
β Actin	TAC AAC CTC CTT GCA GCT CC GGA TCT TCA TGA GGT AGT CAG TC	620 bp	Raff <i>et al.</i> 1997

GAPDH, glyceraldehyde-3-phosphate dehydrogenase

Exposure levels at excitation wavelengths of 340 and 380 nm were chosen to produce images well below saturated levels and to optimize ratios. A 60 min loading time of fura-2 AM generally required exposure times of 0.03 s at 340 nm and 0.01 s at 380 nm, which subsequently resulted in a baseline ratio close to 0.7. Ratios were calculated from the mean intensity of pixels within a software-defined region of interest (ROI) within the cell, chosen from the somatal region of the taste receptor cell. Ratios were background subtracted. The mean intensity from a background ROI was subtracted from the mean intensity value of pixels within the cellular ROI for each wavelength. Pseudocolour was subsequently applied to grey-scale images of the resulting ratio values calculated from background-subtracted 340 nm and 380 nm images. Baseline ratio values, to which stimulated ratio values were compared, were calculated as mean values of five to seven data points acquired prior to stimulus application at the rate of one point per minute.

RT-PCR reactions

Total cellular RNA was isolated from adult brain, heart, lung, adipose tissue, liver, kidney and lingual epithelial tissues containing circumvallate or foliate papilla using a Totally RNA Isolation Kit (Ambion, Austin, TX, USA) according to the manufacturer's instructions (Invitrogen, Carlsbad, CA, USA). Tissue samples were carefully and quickly removed from the

animal, cleaned of adhering tissues, and were immediately either snap frozen and stored at -80°C or homogenized in the kit's denaturing buffer. The RT was performed on the RNA previously digested with DNase I, Amp Grade (Invitrogen), using Superscript II RNase H-Reverse Transcriptase (Invitrogen) according to the manufacturer's instructions. Recombinant RNasin (Promega, Madison, WI, USA) was also added to the reaction as an RNase inhibitor.

The DNA amplification was then performed using 1 μl of cDNA, Platinum *Taq* DNA Polymerase according to the manufacturer's instructions, and the primer sets are described in Table 1. The PCR products were separated by gel electrophoresis in a 1.5% agarose gel containing $0.5 \mu\text{g ml}^{-1}$ ethidium bromide, observed under UV light and photographed. To verify the specificity of the bands, PCR products were either purified by a Concert Rapid PCR Purification System (Invitrogen) and directly sequenced, or cloned (Original TA Cloning Kit, Invitrogen) and sequenced at the Plant-Microbe Genomics Facility at The Ohio State University. The identity of the bands was confirmed with a BLAST search at the NCBI.

Immunocytochemistry

Prior to immunocytochemical analysis, rats were injected i.p. with the monoamine oxidase inhibitor pargyline-HCl 200 mg kg^{-1}

(MAO-B; Rajaofetra *et al.* 1992). After 2 h, animals were anaesthetized and then perfused intracardially with 0.1 M cacodylate buffer containing 1 % sodium metabisulfite (SMB) at pH 6.2, followed by a fixative containing 2.5 % glutaraldehyde and 1 % SMB in 0.1 M cacodylate buffer (pH 7.5). The circumvallate and foliate papillae were excised, blocked, post-fixed in the same fixative for 5 h at 4 °C and then embedded in paraffin following routine methods. Coronal sections were cut at a thickness of 8 μm and collected onto gelatin-coated slides. Sections were dewaxed, rehydrated, washed in Tris-SMB buffer (Tris 0.05 M and SMB 0.85 % pH 7.5) for 30 min and then incubated in sodium borohydride (0.1 M in Tris-SMB) for 10 min. After a thorough rinsing in Tris-SMB for 1 h, sections were processed for immunocytochemistry. Sections were pre-incubated for 1 h at room temperature (RT) in a blocking solution consisting of 5 % normal goat serum (NGS) and 0.2 % Triton X-100 (TX) in Tris-SMB, and then incubated in a commercially available primary antiserum raised in rabbit against noradrenaline conjugated to bovine serum albumin by glutaraldehyde (Chemicon International, Temecula, CA, USA) diluted to 1:100 or 1:200 in Tris-SMB containing 1 % NGS and 0.2 % TX for 36 h at 4 °C. After several rinses in PBS containing 0.01 % TX (PBS-TX), sections were incubated for 2 h at RT in secondary biotinylated goat-anti-rabbit IgG diluted to 1:400 in PBS-TX, rinsed in PBS-TX and then incubated for 1 h in avidin-biotin-peroxidase complex (Vectastain 'Elite ABC' kit, Vector Laboratories) at a dilution of 1:50 in PBS-TX. Tissue-bound peroxidase was visualized by incubating sections in a freshly prepared solution of 0.05 % 3,3'-diaminobenzidine tetrahydrochloride (in 0.05 M Tris buffer, pH 7.6) containing 0.01 % hydrogen peroxide for 3 min. Subsequently, sections were rinsed in distilled water, dehydrated, cleared in xylene and then coverslipped with Permount. Positive immunoreactivity was seen as dark brown reaction product. For experiments using indirect immunofluorescence, sections were incubated for 36 h at 4 °C in the same primary antiserum used above but diluted to 1:10 in Tris-SMB containing 1 % NGS and 0.2 % TX. After several rinses in PBS, sections were incubated for 1.5 h at RT in Cy3-conjugated goat anti-rabbit IgG (Jackson ImmunoResearch Laboratories, West Grove, PA, USA) at a dilution of 1:800. Slides were mounted in Cytoseal 60 (Electron Microscopy Sciences, Washington, PA, USA), and visualized with the aid of an epifluorescence microscope. Using either technique, omission of either primary antibody or secondary antibody eliminated staining.

RESULTS

Noradrenaline inhibits the outward potassium current in taste receptor cells

The addition of low concentrations of noradrenaline to the bathing solution caused an inhibition of outward potassium current in many tested taste receptor cells. Figure 1A illustrates a family of current traces recorded using the whole-cell configuration that were evoked by a series of command pulses in 10 mV increments from a holding potential of -80 mV. In this cell, application of 50 μM noradrenaline reduced the outward current by approximately 23 % (measured from -80 mV to $+90$ mV). The current-voltage relationship of five similar cells to 50 μM noradrenaline is presented in Fig. 1B. Currents were inhibited at all suprathreshold potentials.

Some voltage dependence of the inhibition is evident at higher command potentials where the percentage inhibition increases slightly with increasing command potentials. Data for six concentrations of noradrenaline application, ranging from 0.01 to 100 μM , are summarized in Fig. 1C. The number of cells contributing to each data point is presented in parenthesis. Most of these data were recorded using the perforated-patch technique. Responsive cells showed a strong inhibition to low concentrations of noradrenaline, with concentrations as low as 0.1 μM producing almost maximal inhibitions. Defining a non-responsive cell as one whose inhibition was less than 10 %, 9 out of 14 cells (64 %) responded to 0.1 μM noradrenaline, 22 out of 35 cells (63 %) responded to 1 μM noradrenaline, 15 out of 31 cells (48 %) responded to 10 μM noradrenaline, 26 out of 40 tested cells (65 %) responded to 50 μM noradrenaline and 30 out of 39 cells (77 %) responded to 100 μM noradrenaline. The response magnitude of the potassium currents in the non-responsive cells was 96.9 ± 0.6 % ($n = 57$ cells) and is represented as the filled circle on the left of Fig. 1C. Mean values for the percentage remaining current for tested concentrations of 0.1–100 μM were statistically different from the mean value of non-responsive cells (** $P < 0.001$, Student's one tailed t test). That only subsets of cells responded to noradrenaline is consistent with the usual heterogeneous nature of taste receptor cells. The stability of the current magnitudes of these cells over the recording session attests to the stability of the preparation and suggests that the responses were initiated by receptor-mediated mechanisms and are not due to run down of the currents with time.

The β -receptor agonist isoproterenol (ISP) inhibits the potassium current

Previous studies (e.g. Herness *et al.* 1997) have reported that application of cAMP or cAMP analogues to posterior rat taste receptor cells results in protein kinase A-mediated inhibition of outward potassium currents that is similar in both magnitude and time course to those produced by noradrenaline. Since β -adrenergic receptors operate via the cAMP second messenger system, mediation of the noradrenaline inhibition of potassium currents by β -adrenergic receptors was investigated with the β -agonist ISP. Application of 50 μM ISP resulted in inhibition of outward currents similar to that produced by noradrenaline (Fig. 2A, recorded using the whole-cell configuration) in terms of the overall magnitude of the inhibition, the voltage dependence of the inhibition and the temporal aspects of the rate of rise of the current activation. ISP-mediated inhibition was dose dependent (0.1–100 μM ; Fig. 2B; recorded using the perforated-patch technique) and produced approximately the same maximal effect as noradrenaline. The magnitude of non-responsive cells is indicated by the filled circle (96.2 ± 1.1 %; $n = 16$). Mean values for ISP concentrations

of $1 \mu\text{M}$ and greater were statistically significant when compared to the mean value of the non-responsive cells ($*P < 0.005$; $**P < 0.001$).

To ensure that ISP effects were mediated by β receptors (e.g. as opposed to bitter receptors; drugs commonly taste bitter to humans), ISP-induced inhibition was tested in the presence of the β antagonist propranolol. Prior to these experiments, four concentrations of propranolol were tested alone to ensure that propranolol itself was without effect. The magnitudes of outward potassium current (reported as percentage of remaining current) were $99.7 \pm 2\%$ for $0.2 \mu\text{M}$ ($n = 31$ cells); $105 \pm 5\%$ for $1 \mu\text{M}$ ($n = 11$); $79.5 \pm 7\%$ for $10 \mu\text{M}$ ($n = 12$); and $56.3 \pm 7\%$ for $100 \mu\text{M}$ ($n = 14$) propranolol. Thus, the chosen concentration of $0.2 \mu\text{M}$ propranolol was well below the threshold for inhibition of the potassium current. To test whether propranolol could block the ISP response (Fig. 2C), cells were first exposed to $50 \mu\text{M}$ ISP, rinsed, then exposed to $0.2 \mu\text{M}$ propranolol followed by $50 \mu\text{M}$ ISP in

$0.2 \mu\text{M}$ propranolol. In 20 tested cells, ISP alone reduced the current to $72 \pm 3\%$ of its original magnitude, which was statistically significant when compared to control values ($P < 0.001$), whereas after propranolol, ISP reduced the current to $95 \pm 0.2\%$ of its original value, which was not significant when compared to control values. Moreover, the mean value of the ISP/propranolol group was statistically significant when compared to the mean value of ISP-induced inhibition ($P < 0.001$). These data suggest that ISP is ineffective in the presence of the β -blocker.

Alpha agonists were similarly effective in reducing the outward potassium current

The presence of α receptors was investigated with the application of either the $\alpha 1$ agonist phenylephrine or the $\alpha 2$ agonist clonidine using the perforated-patch technique. Both agonists were effective in reducing the outward potassium current. Phenylephrine inhibited 36% of tested cells, whereas clonidine inhibited 74% of tested

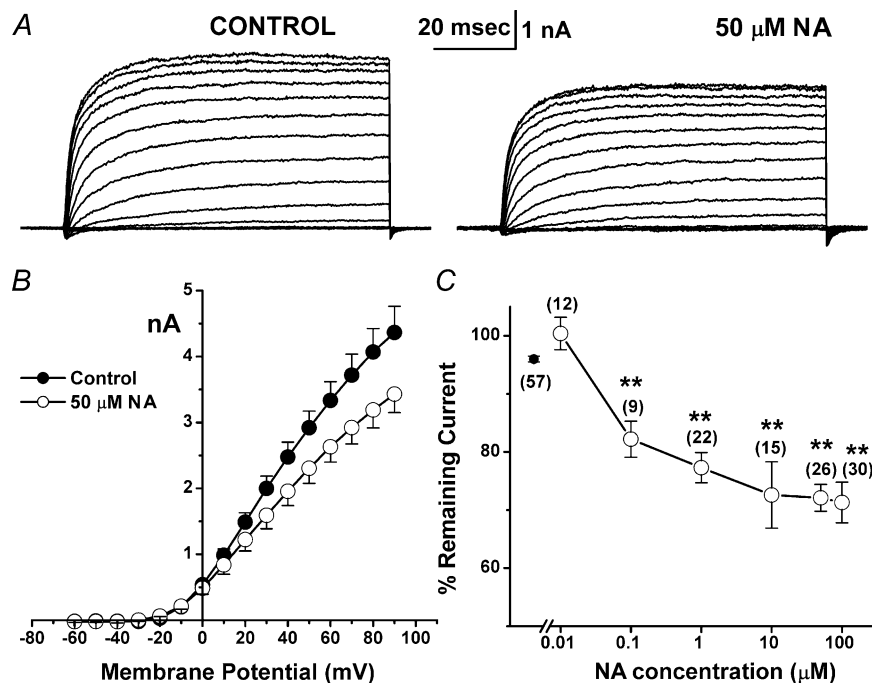


Figure 1. Noradrenaline reduces outward potassium currents in dissociated rat taste receptor cells

A, a family of whole-cell currents recorded from a dissociated taste receptor cell in extracellular fluid (ECF) and ECF containing $50 \mu\text{M}$ noradrenaline (NA). Outward potassium currents were reduced by approximately 20% in the presence of exogenous noradrenaline. The cell was held at -80 mV and command pulses in 10 mV increments were applied to a final potential of $+90$ mV. As is typical for these cells, outward potassium currents are much larger in magnitude than inward sodium currents. B, a typical current–voltage relationship is illustrated for five cells that had similar control magnitudes of outward currents (●) and were responsive to noradrenaline (tested at $50 \mu\text{M}$; ○). Potassium currents were inhibited at all suprathreshold voltages, although inhibition was greater at more depolarized membrane potentials. C, dose–response profile for noradrenergic inhibition of potassium currents. Six concentrations of noradrenaline, ranging from 0.01 to $100 \mu\text{M}$, were applied (○). The dose–response curve produced a maximum effect of about 25% inhibition at concentrations of $10 \mu\text{M}$ and higher. Data are presented as means \pm S.E.M. and the number of cells is indicated in parentheses. Most cells were recorded with the perforated-patch technique. The data point at the far left (●) represents the post-application mean magnitude of the 57 cells tested with different concentrations of noradrenaline that were classified as non-responders. $**P < 0.001$.

cells. A sample record of the inhibition of outward potassium currents produced by 100 μM clonidine is presented in Fig. 3A, which was similar in magnitude to that produced by either noradrenaline or ISP. At the 100 μM test concentration, the magnitude of the outward potassium currents was $85.5 \pm 1\%$ (20 out of 55 tested cells) for phenylephrine and $80 \pm 1.4\%$ (55/74) for clonidine (Fig. 3B). Both groups were statistically significant when compared to control values (** $P < 0.001$). In general, the time course of recovery for the α agonists was faster than that observed for β agonists.

Experiments with α antagonists were not possible as we could not find a concentration of antagonist that would be effective for blocking α receptors without itself reducing potassium currents. For example, yohimbine, an α_2 antagonist commonly used at concentrations of 1–10 μM , is an effective bitter stimulus in the rat (Dahl *et al.* 1997). We tested yohimbine for inhibition of outward potassium current and measured the percentage remaining current:

$97.5 \pm 3\%$ for 0.1 μM ($n = 11$ cells); $89.2 \pm 3\%$ for 1 μM ($n = 15$); $88.6 \pm 4\%$ for 10 μM ($n = 17$); $57.8 \pm 8\%$ for 50 μM ($n = 9$); $42.3 \pm 4\%$ for 100 μM ($n = 16$). Thus, yohimbine probably acts as a bitter agonist at the same concentrations required as an α antagonist.

In 17 tested cells, application of both α (clonidine) and β (ISP) agonists was tested. Fourteen cells responded to one or both agonists, while 3 cells responded to neither. Of these 14 responding cells, 2 responded only to ISP, 5 responded only to clonidine and 7 responded to both agonists. Overall, 9 responded to ISP (53%) and 12 responded to clonidine (70%), which agrees well with our previous results. These preliminary results suggest that the expression pattern of α and β receptors at a cellular level are heterogeneous, with some cells expressing only β receptors, some only α receptors, and some cells expressing both. However, actions of α receptor agonists at other receptor subtypes cannot yet be excluded.

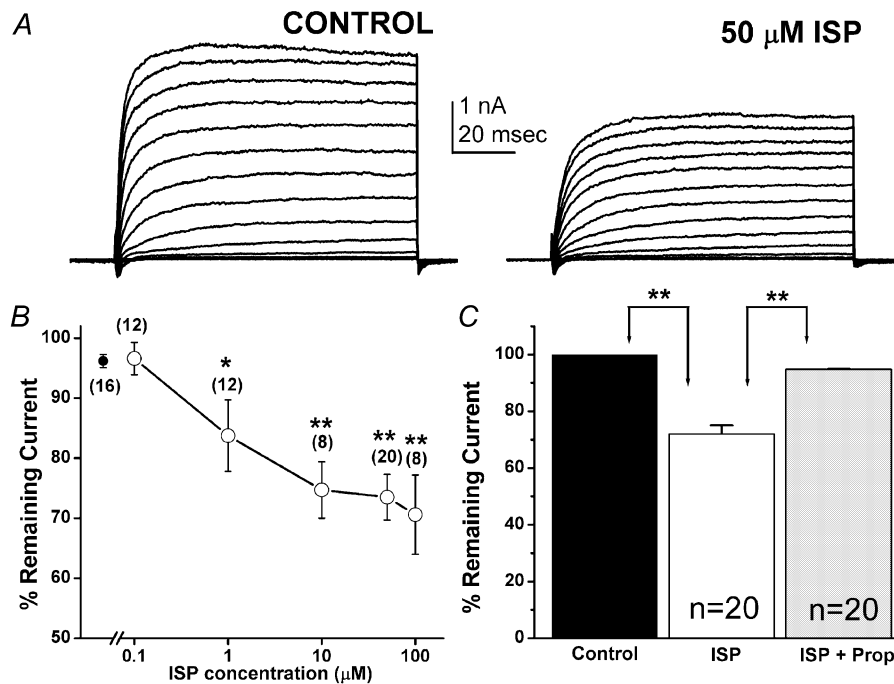


Figure 2. Inhibition of potassium currents by noradrenaline is mimicked by the β agonist isoproterenol (ISP)

A, a family of whole-cell currents recorded in standard ECF solution and ECF solution containing 50 μM ISP. ISP application produced a strong inhibition of the outward potassium currents, approximately 30% in this cell. B, concentration–response profile for the ISP inhibition of potassium currents. Data are presented as means \pm S.E.M. (○) and the number of cells for each point is indicated in parentheses. Most of these cells were recorded with the perforated-patch technique. Tested concentrations of ISP above 0.1 μM were effective in reducing the magnitude of the outward potassium currents. The data point at the far left (●) represents the mean magnitude of potassium current in cells that did not respond to ISP. The inhibition produced by ISP was very similar in magnitude to that produced by NA. * $P < 0.005$; ** $P < 0.001$. C, summarized data of potassium-current inhibition presented in histogram form. The magnitude of the current to a test pulse (–80 mV to +90 mV) was reduced to $72 \pm 3\%$ of its amplitude in the presence of 50 μM isoproterenol, and to $95 \pm 0.2\%$ when exposed to an isoproterenol and propranolol (Prop) mixture ($n = 20$ cells each). Thus, propranolol could successfully eliminate the ISP response, suggesting that the ISP inhibition is mediated by β receptors rather than by another mechanism (such as bitter receptors). ** $P < 0.001$ when comparing the means of the groups indicated by arrows.

Since some α adrenergic receptors are coupled to the inositol trisphosphate second-messenger system, and hence intracellular calcium, the effect of noradrenaline, clonidine or phenylephrine was tested on dissociated taste receptor cells using ratiometric calcium imaging with the fluroprobe fura-2. The drug was applied focally to individual cells via pipette administration. Nine of the 52 tested cells responded to 100 μM noradrenaline with an elevation of intracellular calcium. Cells also responded to α agonists with elevations of intracellular calcium. A sample response to phenylephrine is presented in Fig. 4A. In all cases, elevations of intracellular calcium were transient (Fig. 4B). Often, second applications of noradrenaline or α agonist were ineffective, although subsequent tests with the bitter tastant caffeine (10 mM), which we have previously demonstrated to be an effective stimulator of intracellular calcium (Zhao *et al.* 2002), remained robust, suggesting the cell remained in a physiologically responsive state. This phenomenon could represent either desensitization or the selective depletion of physiologically segregated local intracellular calcium pools. After noradrenaline application, cells were subsequently tested with 100 μM clonidine or 100 μM phenylephrine (Fig. 4C). Five of the 52 cells responded to phenylephrine, whereas 4 of the 52 cells responded to clonidine. Two of these cells responded to both agonists.

Overall, fewer cells responded with increases of intracellular calcium than observed to respond with inhibitions of potassium current. Hence, using patch-clamp or calcium-imaging measures, cells appeared to express α and β receptors in a heterogeneous manner.

Inwardly rectifying potassium currents are unaffected by adrenergic stimulation

K_{IR} are expressed ubiquitously, are major contributors to the resting potential in taste receptor cells (Sun & Herness, 1996), and are therefore logical candidates in examining putative adrenergic effects on electrical excitability. Applied at concentrations ranging from 50 to 500 μM , no discernible actions of exogenous noradrenaline could be noted on the magnitude or time course of the recorded current traces (Fig. 5A; whole-cell configuration). The current–voltage plots show summarized data from five cells. Similarly, exogenously applied analogue of cAMP, 8cpt-cAMP, or application of the adenylate cyclase activator forskolin was without effect on K_{IR} (Fig. 5B). The current–voltage plots show summarized data from six cells. No differences were noted for either pharmacological manipulation. Response magnitudes to the test pulse to -160 mV were $97.4 \pm 4.9\%$ for noradrenaline ($n = 5$ cells), $95 \pm 2.6\%$ for 8cpt-cAMP ($n = 5$ cells) and $103 \pm 1.1\%$ for forskolin ($n = 2$ cells) of their baseline values.

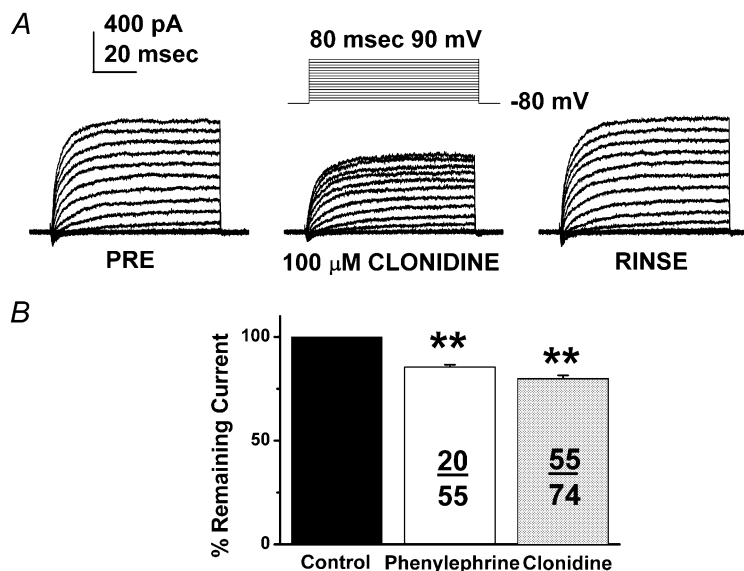


Figure 3. α agonists are also effective in inhibiting outward potassium currents

A, sample currents recorded prior to, during and after application of the α_2 agonist, clonidine using the perforated-patch technique. Similar to β stimulation, clonidine was effective in reducing the magnitude of the outward potassium currents without noticeable effect on their time course. The effect was reversible and somewhat more evident at more depolarized command potentials. B, histogram of the inhibitory effect of 100 μM phenylephrine (an α_1 agonist) or 100 μM clonidine (an α_2 agonist) on the outward potassium current. Data are presented as the amount of current, induced by a test pulse from -80 mV to $+90$ mV, persisting after drug application. Phenylephrine reduced the potassium current to $85.5 \pm 1.1\%$ of its original magnitude. It was effective in 20 out of 55 tested cells. Clonidine reduced the potassium currents to $80 \pm 1.5\%$. It was effective in 55 out of 74 tested cells. These magnitudes of inhibition are similar to those produced by either noradrenaline or isoproterenol. Both groups were statistically significant when compared to control values (** $P < 0.001$).

To test if K_{IR} could be altered by other exogenous means, G-protein modulators were tested, since many K_{IR} channels are directly activated by G-proteins without the intervention of cytosolic messengers (formerly referred to as GIRK family but now as K_{IR3}). The GTP analogues $GTP\gamma S$, which results in irreversible activation of G-proteins, and $GDP\beta S$, which serves as a control, were tested. $GTP\gamma S$ was an effective inhibitor of K_{IR} . Sample

records of K_{IR} with standard ICF, ICF containing $500 \mu M$ $GTP\gamma S$, or $500 \mu M$ $GDP\beta S$ are presented in Fig. 5C both immediately after breaking into (1 min) and 40 min after obtaining a whole-cell configuration. Currents were strongly inhibited in the presence of $GTP\gamma S$ over all tested potentials. Typically, an initial transient was relatively unaffected, whereas steady-state currents were reduced in magnitude up to 50%. Summarized results are presented

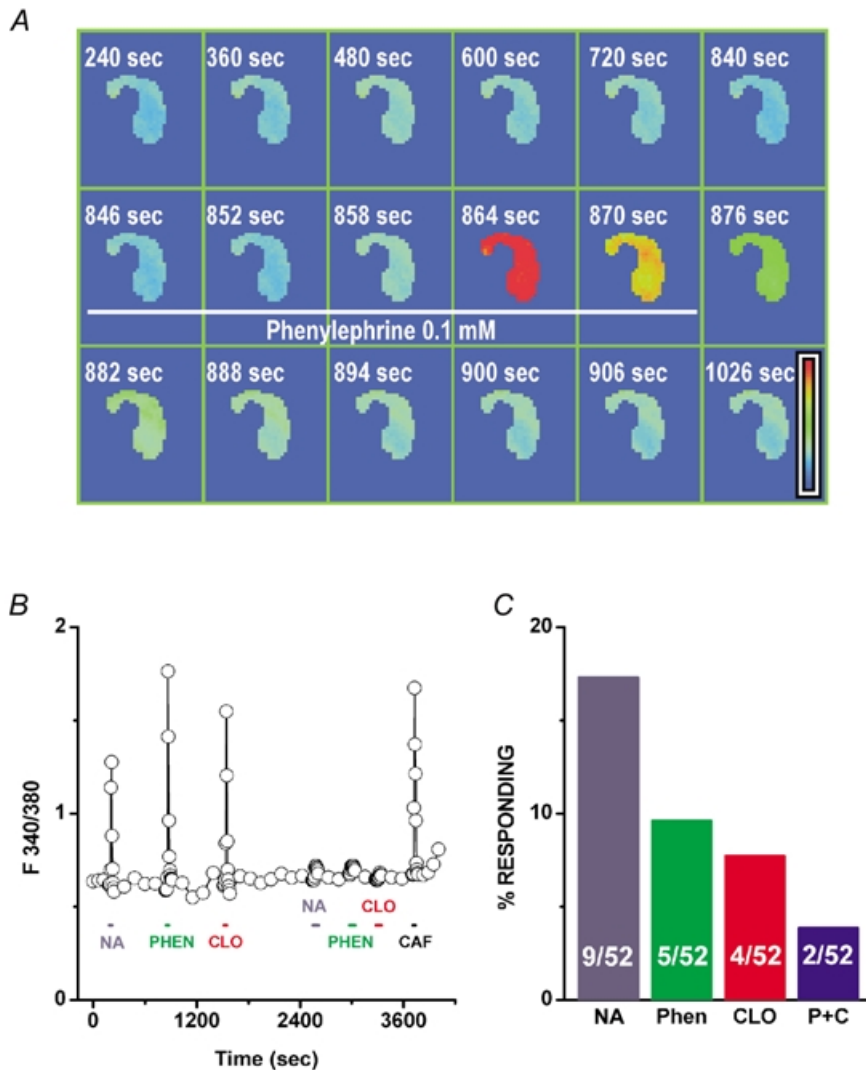


Figure 4. α agonists are effective at elevating intracellular calcium in taste receptor cells

A, a pseudocolour representation of a single taste receptor cell, imaged using a ratiometric procedure with fura-2, before, during and after application of $100 \mu M$ phenylephrine. Images represent ratio values calculated from raw intensity values obtained at 340 and 380 nm excitations. The scale bar (lower right) indicates relative calcium levels, with red as high and blue as low. Images were acquired at the indicated times. Phenylephrine application, delivered via a pipette positioned close to the cell, began at 846 s in this record and its duration is indicated by the solid white bar. Phenylephrine increased intracellular calcium quickly after its application and was reversed with washout. *B*, a diagrammatic representation of ratio values obtained from the cell illustrated in *A* to varying stimuli. This cell responded to $100 \mu M$ NA, $100 \mu M$ phenylephrine (PHEN), and $100 \mu M$ clonidine (CLO) with elevations of intracellular calcium. The durations of each stimulus application are indicated by the filled bars. As is typical, the cell did not respond to a second application of each stimulus, yet it responded strongly to a fourth stimulus, 10 mM Caffeine (CAF). *C*, histogram displaying the percentage of 52 tested cells that responded to either $100 \mu M$ NA, $100 \mu M$ phenylephrine (Phen), or $100 \mu M$ clonidine (CLO). Two cells (labelled P + C) responded to both phenylephrine and clonidine.

in Fig. 5C. Response magnitudes to a test pulse were stable over a 40 min period when the intracellular pipette contained either normal ICF solution (○, $n = 5$) or normal ICF with 500 μM GDP βS (□, $n = 15$), but dropped precipitously when ICF contained 500 μM GTP γS (●, $n = 8$). Data from the GTP γS group were statistically significant when compared to the ICF control group ($*P < 0.05$, $**P < 0.01$), whereas none of the GTP γS group data achieved statistical significance when compared to ICF control.

Multiple adrenoceptors are expressed in the lingual epithelium

The expression of messenger RNA for various subtypes of adrenoceptors in lingual epithelium was tested with RT-PCR experiments using oligonucleotide primers specific for 10 different subtypes of adrenergic receptor (sequences

and references listed in Table 1). Total RNA was extracted from lingual tissue epithelium of combined circumvallate and foliate papillae or from various control tissues and used for production of template cDNA. Primers were tested using template cDNA derived from RNA extracted from positive control tissue (cortex, heart, liver and adipose tissue). Controls for DNA contamination and PCR carryover were performed by omitting the reverse transcriptase (RT $-$) and by exclusion of RNA from the RT-PCR reaction; all produced no PCR products (RT $-$ illustrated). Amplifications of two housekeeping genes, glyceraldehyde-3-phosphate dehydrogenase (GAPDH) and β -actin and of α -gustducin, a G-protein that specifically expressed in taste receptor cells, were employed as positive controls. The PCR product using primers specific for α -gustducin was purified and sequenced to verify its identity.

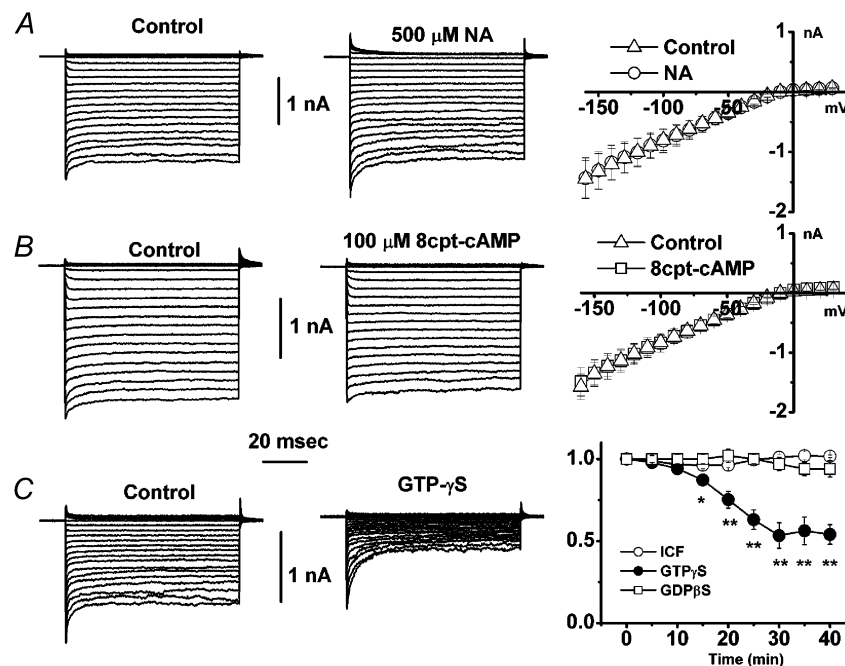


Figure 5. Noradrenaline and cAMP are ineffective in altering the magnitude of inwardly rectifying potassium currents

A, inwardly rectifying potassium currents recorded prior to and during administration of 500 μM noradrenaline using the whole-cell recording technique. Noradrenaline was ineffective in altering the magnitude of these currents. Summated data (mean \pm S.E.M.) from five cells in the form of a current-voltage plot are presented at the far right. The current-voltage relationships in the presence or absence of noradrenaline were indistinguishable. B, inwardly rectifying potassium currents prior to and during administration of 100 μM 8cpt-cAMP using the whole-cell configuration. As with noradrenaline application, 8cpt-cAMP was ineffective in altering the magnitude of these currents. Summated data from four cells are presented in the current-voltage plot at the right. C, inwardly rectifying potassium currents from two different cells are presented 40 min after breaking into whole-cell configuration using either standard pipette solution (pseudo-intracellular fluid, ICF), or ICF containing 500 μM GTP γS (an irreversible activator of G-proteins). Note that currents were strongly inhibited when the recording pipette contained GTP γS . To the right are summarized data of inhibition of the inwardly rectifying potassium current produced by G-protein activation. Mean data (the normalized current magnitude produced by a test pulse to -160 mV) are presented using pipettes filled with standard ICF (○; control), 500 μM GTP γS (●), or 500 μM GDP βS (□; an inactive control). Each data point represents the mean of 4–15 cells. Current magnitudes were stable for the 40 min test period for using pipettes with either standard ICF or ICF containing GDP βS , whereas GTP γS strongly inhibited the inwardly rectifying potassium current. Significantly different from the ICF group at $*P < 0.05$, $**P < 0.01$.

PCR reactions with primers for adrenergic receptor subtypes yielded cDNA fragments of the correct size for 9 out of 10 tested primers sets. These were $\alpha 1a$ (212 bp), $\alpha 1b$ (300 bp), $\alpha 1c$ (251 bp), $\alpha 1d$ (304 bp), $\alpha 2a$ (312 bp), $\alpha 2b$ (456 bp), $\alpha 2c$ (425 bp), $\beta 1$ (376 bp) and $\beta 2$ (343 bp). No bands using primers specific for $\beta 3$ receptors were observed. The amplified products were cloned and sequenced to confirm their identity. The sequences were analysed by BLAST search of GenBank database at NCBI (National Center for Biotechnology Information; www.ncbi.nlm.nih.gov) and were found to correspond to published sequences for each corresponding adrenergic receptor. These data demonstrate the expression of multiple adrenergic receptors to lingual epithelium. Since the excised starting material also contains non-gustatory

epithelial cells, these PCR results, considered alone, cannot conclusively localize expression of all receptor subtypes to taste receptor cells. However, they are in agreement with physiological data on single taste receptor cells that corroborate expression of both α and β receptors.

Immunocytochemical localization of noradrenaline to taste receptor cells

To investigate whether taste receptor cells could serve as the endogenous source of noradrenaline, immunocytochemistry was performed on rat circumvallate and foliate papillae using a commercially available antibody generated in rabbit against noradrenaline conjugated by glutaraldehyde to bovine serum albumin (Chemicon). Two visualization techniques were employed: the avidin-biotin technique using diaminobenzidine as the

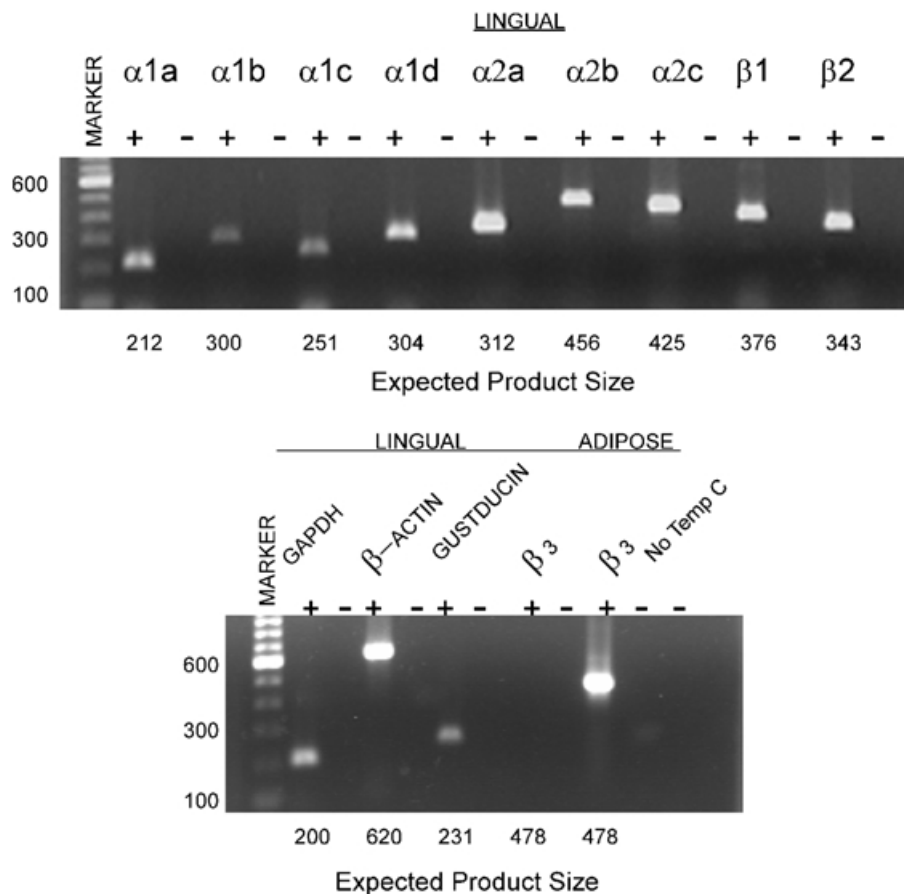


Figure 6. RT-PCR experiments performed on RNA isolated from lingual epithelium using primers specific for adrenergic receptors

A, PCR-amplified products from cDNA reverse transcribed from RNA isolated from the lingual epithelium of circumvallate and foliate papillae. Oligonucleotide primers specific for ten different adrenergic receptors ($\alpha 1a$, $\alpha 1b$, $\alpha 1c$, $\alpha 1d$, $\alpha 2a$, $\alpha 2b$, $\alpha 2c$, $\beta 1$, $\beta 2$ and $\beta 3$) were run in separate reactions and the products run on agarose gel electrophoresis. The expected product size of each reaction is listed below each lane. To control for genomic contamination, reactions with each primer set were run in parallel with (RT+) and without (RT-) inclusion of reverse transcriptase. Results from these reactions are illustrated in adjacent lanes. Products were observed in RT+ reactions of all primer sets with the exception of the $\beta 3$ primer set. No products were observed in any of the RT- reactions. Molecular markers from 100 to 700 bp (in 100 bp increments) are in the far left lane. B, PCR-generated products using primers specific for $\beta 3$ receptors using cDNA templates derived from lingual tissue (with or without reverse transcriptase) or adipose tissue (a positive control). The PCR product was only observed with the positive control tissue.

chromophore, and an immunofluorescence technique with a Cy3-conjugated secondary antibody. In an attempt to enhance antigen concentration, animals were injected I.P. with the monoamine oxidase inhibitor pargyline-HCl 200 mg kg^{-1} (MAO-B) 2 h prior to killing. The adrenal medulla was processed as a positive control tissue. Negative controls included omission of the primary antibody and are illustrated at the far right of Fig. 7A and B.

Subsets of immunopositive cells were observed in most taste buds examined using either visualization technique (Fig. 7). Immunoreactivity was present throughout the cytoplasm; nuclei were clear and devoid of reaction product. Several cells were observed in single taste buds and positive cells typically had large round nuclei suggestive of light cells. Immunostaining was also present within the connective tissue adjacent to the gustatory epithelium. This staining could represent the presence of adrenergic fibres (e.g. Paparelli *et al.* 1986, 1988), but its presence may also represent non-specific antibody staining.

To estimate the number of adrenergic taste receptor cells per bud, immunopositive cells were counted in 34 taste buds from 8 different foliate sections. The total of 119 labelled cells produced an average of 3.5 labelled cells per cross-sectioned taste bud. Since a single taste bud (approximately $50 \mu\text{m}$ in diameter) may encompass about 6 sections in our experiments, and assuming that different cross-sectional areas of sectioned taste buds were equally represented in our analysis, we estimate that an individual taste bud might contain up to 20 noradrenaline-expressing taste receptor cells. This estimate is probably a high approximation, since taste buds with large cross-sectional areas were easier to count than smaller cross-sections and hence are likely to be represented more often than marginal cross-sections.

DISCUSSION

Many significant gaps exist in the understanding of how gustatory information is processed at the peripheral level. Although aspects of transduction mechanisms in response

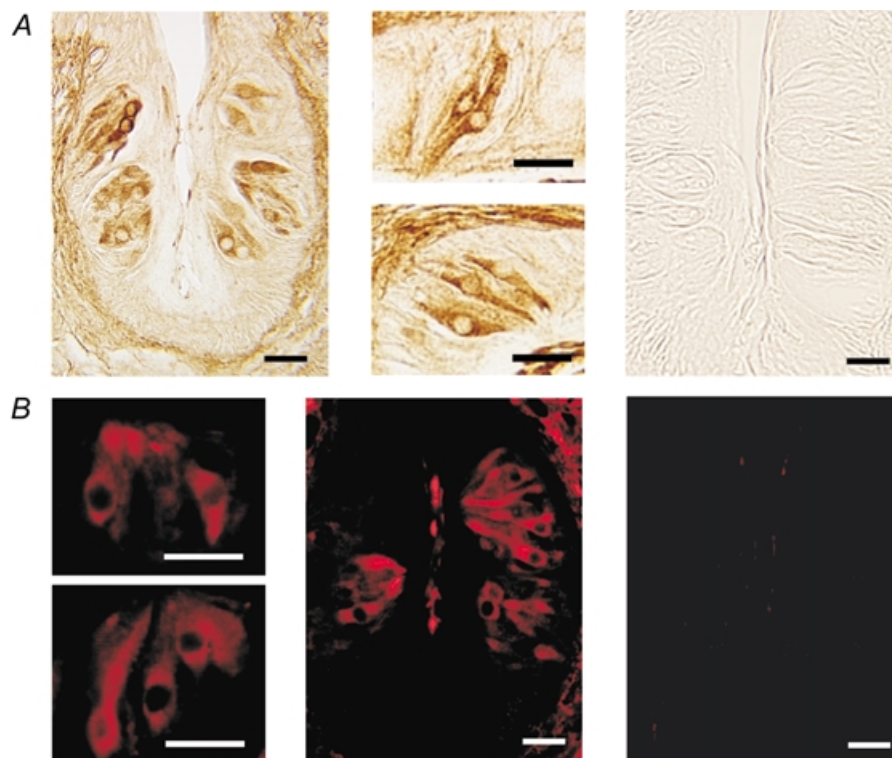


Figure 7. Immunocytochemical localization of noradrenaline to the posterior taste receptor cells of the rat tongue

A, sample sections of foliate papillae immunostained with an antibody directed against noradrenaline. Sectioned tissue was reacted using an avidin-biotin technique with diaminobenzidine as the chromophore. Note the presence of several darkly stained taste receptor cells within the taste buds. The photomicrograph at the far right is a negative control section with omission of the primary antibody. Scale bars are $20 \mu\text{m}$. B, examples of sample taste buds containing taste receptor cells immunopositive for NA-like immunoreactivity from foliate papillae. Tissue sections were reacted using an immunofluorescence technique with a Cy3-conjugated secondary antibody. Many taste receptor cells displayed intense fluorescent labelling in their cytoplasm while their nuclei remained clear and were devoid of any positive signal. The photomicrograph at the far right is a negative control section with omission of the primary antibody. Scale bars are $20 \mu\text{m}$.

to chemical stimulation are being resolved (e.g. Herness & Gilbertson, 1999; Gilbertson *et al.* 2000; Lindemann, 2001), less attention is being paid to events occurring after excitation of the taste receptor cell. A simple story of one taste cell exciting a single afferent nerve belies both the complexity of the peripheral gustatory system and its extant physiological data. That evidence exists for more than one type of neurotransmitter within rat taste buds (e.g. Nagai *et al.* 1996; Yamamoto, 1998), and evidence that taste receptor cells, in addition to afferent nerve fibres, respond to transmitters, strongly favours cell-to-cell communication as a basis for information processing within the taste bud. Collectively, the present data suggest that taste receptor cells possess all the necessary substrates to use noradrenaline for cell-to-cell communication.

Prior evidence for noradrenaline as a neurotransmitter in the gustatory system

Prior evidence for noradrenaline within taste buds has been indirect and somewhat conflicting. Earliest suggestions that noradrenaline operates as a neurotransmitter in the mammalian gustatory system came from histofluorescence studies (Gabella, 1969; Geerdink & Drukker, 1973; Takeda & Kitao, 1980; Takeda *et al.* 1982) that led investigators to believe that subsets of taste cells in rabbits and mice could be adrenergic. These early studies could not differentiate between the monoamine noradrenaline and serotonin; moreover, histofluorescence was enhanced by prior injection of a precursor of either of these substances (L-3,4-dihydroxyphenylalanine (L-DOPA) or 5-hydroxytryptophan, respectively). Other studies (Cano *et al.* 1982a, b), using a biochemical assay to differentiate between serotonin and noradrenaline, confirmed the presence of both monoamines in the gustatory papillae. Somewhat in contrast, examinations by Paparelli *et al.* (1986, 1988) suggest that noradrenaline is in the adrenergic nerve fibres that surround the taste bud (perigemmal fibres that innervate the core of fungiform, foliate or circumvallate papillae). They speculated that adrenergic influences on taste responses might be secondary to changes in the local vasculature of the papilla. These anatomical studies were complemented by physiologic studies. In the frog, gustatory nerve responses are enhanced by noradrenaline. Morimoto & Sato (1982) perfused the lingual artery with catecholamines and observed that amines enhanced spontaneous glossopharyngeal nerve responses. Nerve responses to stimuli were enhanced by noradrenaline but not dopamine, whereas injection of monoamine-depleting agents, suppressed responses to taste stimuli. Using the same preparation, Nagahama & Kurihara (1985) confirmed the enhancement of taste responses by noradrenaline and showed that this enhancement was suppressed if desipramine and imipramine, both inhibitors of noradrenaline uptake, were added to the perfusing solution. Both studies concluded that noradrenaline plays

a significant role in afferent synaptic transmission in the frog taste organ.

Although these early findings were suggestive, two recent reviews on neurotransmission in taste buds (Nagai *et al.* 1996; Yamamoto *et al.* 1998) independently concluded that the existing data for noradrenaline was too vestigial in its identifying criteria to conclude that catecholaminergic transmission occurs in the taste bud. Nevertheless, these prior studies do provide a solid and supportive platform for the present work. Adrenergic nerve fibres and taste receptor cells exist in mammalian papillae. The physiological consequences of adrenergic release and consequent modulation of gustatory afferent activity may be the result of either post-synaptic afferent activation and/or cell-to-cell communication in the bud that, in turn, enhances the afferent output.

Physiological consequences of adrenergic stimulation in taste buds

Data presented in this communication establish firmly both the localization and functional role for noradrenaline in taste buds. Moreover, they also confirm the growing notion that neurotransmitters in mammalian taste buds function in cell-to-cell communication.

Subsets of taste receptor cells responded to adrenergic stimulation. Phenotyping these cells will be an important step towards ultimately understanding the role of adrenergic stimulation. In this communication we recorded from a total of 386 taste receptor cells that responded positively to adrenergic stimulation. Of these cells, 321 (or 83%) expressed sodium currents. We have reported previously that 50–75% of rat posterior taste receptor cells express sodium currents (Herness & Sun, 1995). Therefore, there may be some positive correlation between the expression of adrenergic receptors and sodium currents. In addition, we have reported previously that β -receptor stimulation enhances chloride currents in a subset of taste receptor cells. Although it is likely that there will be an overlap between these two groups of cells, it is not presently known with certainty if these are the same or different groups of cells.

Overall, the physiological effects of noradrenaline observed in this study suggest that adrenergic actions occur during a state of excitation. The observed reduction in the outward potassium current by either α - or β -receptor activation would produce an increase in the duration of the action potential, causing the cell to remain in a depolarized state for a protracted period. Increased intracellular calcium as a result of α -receptor stimulation is an additional event correlated with excitation. The lack of action on K_{IR} , a likely mechanism by which a resting cell may be brought into an active state, additionally suggests that adrenergic actions are occurring during active rather than passive phases of electrical excitability in taste

receptor cells. Finally, in the most general of terms, release of a neurotransmitter, such as noradrenaline, would be expected to occur as a result of stimulation.

The interplay between α and β receptors within the taste bud is likely to be complex. Our preliminary data suggest that individual taste receptor cells expressing adrenergic receptors express either α receptors, β receptors, or both. These receptors may act both pre-synaptically and post-synaptically. Furthermore, these actions may potentiate other events occurring during the excitatory process. For example, other tastants and other neurotransmitters may affect cAMP levels or intracellular calcium levels in taste receptor cells.

Among the more pressing issues towards understanding cell-to-cell communication within the taste bud is correlating cell types with transmitters and their receptors. In particular, only a minority of taste receptor cells form synapses within the bud. It is plausible that non-synaptically connected taste receptor cells (e.g. type I or II) could release transmitters to synaptically connected taste receptor cells (e.g. type III), hence allowing a pathway for their stimulus-driven activation to relay meaningful information to the afferent nerve. Moreover, such a mechanism would allow for amplification of the response, since more than one cell could influence the innervated taste receptor cell. How particular stimuli activate unique communication pathways within the bud awaits future experimentation.

REFERENCES

- BIGIANI, A., DELAY, R. J., CHAUDHARI, N., KINNAMON, S. C. & ROPER, S. D. (1997). Responses to glutamate in rat taste cells. *Journal of Neurophysiology* **77**, 3048–3059.
- CAICEDO, A., JAFRI, M. S. & ROPER, S. D. (2000a). In situ imaging reveals neurotransmitter receptors for glutamate in taste receptor cells. *Journal of Neuroscience* **20**, 7978–7985.
- CAICEDO, A., KIM, K. N. & ROPER, S. D. (2000b). Glutamate-induced cobalt uptake reveals non-NMDA receptors in rat taste cells. *Journal of Comparative Neurology* **417**, 315–324.
- CANO, J., LOBERA, B., RODRIGUEZ-ECHANDIA, E. L. & MACHADO, A. (1982a). Influence of innervation on the levels of noradrenaline and serotonin in the circumvallate papilla of the rat. *Journal of Neurobiology* **13**, 1–7.
- CANO, J., MACHADO, A., ROZA, C. & RODRIGUEZ-ECHANDIA, E. (1982b). Effect of testosterone on serotonin and noradrenaline concentrations and taste bud cell number of rat circumvallate papilla. *Chemical Senses* **7**, 109–116.
- CHAUDHARI, N., YANG, H., LAMP, C., DELAY, E., CARTFORD, C., THAN, T. & ROPER, S. (1996). The taste of monosodium glutamate: Membrane receptors in taste buds. *Journal of Neuroscience* **16**, 3817–3826.
- CHAUDHARI, N., LANDIN, A. & ROPER, S. D. (2000). A metabotropic glutamate receptor variant functions as a taste receptor. *Nature Neuroscience* **3**, 113–119.
- DAHL, M., ERICKSON, R. P. & SIMON, S. A. (1997). Neural responses to bitter compounds in rats. *Brain Research* **756**, 22–34.
- FINGER, T. E. & SIMON, S. A. (2000). Cell biology of taste epithelium. In *The Neurobiology of Taste and Smell*, 2nd edn, ed. FINGER, T. E., SILVER, W. L. & RESTREPO, D., pp. 287–314. Wiley-Liss, New York.
- FORT, P. H., MARTY, L., PIECHACZYK, M., EL SABROUTY, S., DANI, C. H., JEANTEUR, P. H. & BLANCHARD, J. M. (1985). Various rat adult tissues express only one major mRNA species from glyceraldehyde-3-phosphate-dehydrogenase multigenic family. *Nucleic Acids Research* **13**, 1431–1442.
- GABELLA, G. (1969). Taste buds and adrenergic fibers. *Journal of the Neurological Sciences* **9**, 237–242.
- GEERDINK, H. G. & DRUKKER, J. (1973). Uptake of l-dopa by cells in the taste buds of the vallate papilla of the mouse. *Histochemie* **36**, 219–223.
- GILBERTSON, T. A., DAMAK, S. & MARGOLSKEE, R. F. (2000). The molecular physiology of taste transduction. *Current Opinion in Neurobiology* **10**, 519–527.
- GOULD, D. J., VIDOVIC, M. & HILL, C. E. (1995). Cross talk between receptors mediating contraction and relaxation in the arterioles but not the dilator muscle of the rat iris. *British Journal of Pharmacology* **115**, 828–834.
- HERNESS, S. & CHEN, Y. (1997). Serotonin inhibits calcium-activated K^+ current in rat taste receptor cells. *NeuroReport* **8**, 3257–3261.
- HERNESS, M. S. & CHEN, Y. (2000). Serotonergic agonists inhibit calcium-activated potassium and voltage-dependent sodium currents in rat taste receptor cells. *Journal of Membrane Biology* **173**, 27–138.
- HERNESS, M. S. & GILBERTSON, T. A. (1999). Cellular mechanisms of taste transduction. *Annual Review of Physiology* **61**, 873–900.
- HERNESS, M. S. & SUN, X. D. (1995). Voltage-dependent sodium currents recorded from dissociated rat taste cells. *Journal of Membrane Biology* **146**, 73–84.
- HERNESS, M. S. & SUN, X. D. (1999). Characterization of chloride currents and their noradrenergic modulation in rat taste receptor cells. *Journal of Neurophysiology* **82**, 260–271.
- HERNESS, M. S., SUN, X. D. & CHEN, Y. (1997). Cyclic AMP and forskolin inhibit potassium currents in rat taste cells by different mechanisms. *American Journal of Physiology* **272**, C2005–2018.
- KIM, D. J. & ROPER, S. D. (1995). Localization of serotonin in taste buds: a comparative study in four vertebrates. *Journal of Comparative Neurology* **353**, 364–370.
- LIN, W. H. & KINNAMON, S. C. (1999). Physiological evidence for ionotropic and metabotropic glutamate receptors in rat taste cells. *Journal of Neurophysiology* **82**, 2061–2069.
- LINDEMANN, B. (2001). Receptors and transduction in taste. *Nature* **413**, 219–225.
- MCLAUGHLIN, S. K., MCKINNON, P. J. & MARGOLSKEE, R. F. (1992). Gustducin is a taste-cell-specific G protein closely related to the transducins. *Nature* **357**, 563–569.
- MORIMOTO, K. & SATO, M. (1982). Role of monoamines in afferent synaptic transmission in frog taste organ. *Japanese Journal of Physiology* **32**, 855–871.
- NAGAHAMA, S. & KURIHARA, K. (1985). Norepinephrine as a possible transmitter involved in synaptic transmission in frog taste organs and Ca dependence of its release. *Journal of General Physiology* **85**, 431–442.
- NAGAI, T., KIM, D. J., DELAY, R. J. & ROPER, S. D. (1996). Neuromodulation of transduction and signal processing in the end organs of taste. *Chemical Senses* **21**, 353–365.
- NELSON, G., CHANDRASHEKAR, J., HOON, M. A., FENG, L., ZHAO, G., RYBA, N. J. P. & ZUKER, C. S. (2002). An amino-acid receptor. *Nature* **416**, 199–202.

- OBATA, H., SHIMADA, K., SAKAI, N. & SAITO, N. (1997). GABAergic neurotransmission in rat taste buds: immunocytochemical study for GABA and GABA transporter subtypes. *Molecular Brain Research* **49**, 29–36.
- PAPARELLI, A., PELLEGRINI, A. & SOLDANI, P. (1988). Noradrenergic innervation of the lingual papillae in certain rodents pre-treated with adriblastin. II. A comparative study on circumvallate and foliate papillae. *Bollettino della Società Italiana di Biologia Sperimentale* **64**, 907–913.
- PAPARELLI, A., SOLDANI, P. & PELLEGRINI, A. (1986). Noradrenergic innervation of the lingual papillae in certain rodents pre-treated with adriblastin. I. Comparative study on the filiform and fungiform papillae. *International Journal of Tissue Reactions* **8**, 527–531.
- RAFF, T., VAN DER GIET, M., ENDEMANN, D., WIEDERHOLT, T. & PAUL, M. (1997). Design and testing of β -actin primers for RT-PCR that do not co-amplify processed pseudogenes. *BioTechniques* **23**, 456–460.
- RAJAOFETRA, N., POULAT, P., MARLIER, L., GEFFARD, M. & PRIVAT, A. (1992). Pre- and postnatal development of noradrenergic projections to the rat spinal cord: an immunocytochemical study. *Brain Research Developmental Brain Research* **67**, 237–246.
- REN, Y., SHIMADA, K., SHIRAI, Y., FUJIMIYA, M. & SAITO, N. (1999). Immunocytochemical localization of serotonin and serotonin transporter (SET) in taste buds of rat. *Molecular Brain Research* **74**, 221–224.
- SCOFIELD, M. A., LIU, F., ABEL, P. W. & JEFFRIES, W. B. (1995). Quantification of steady state expression of mRNA for alpha-1 adrenergic receptor subtypes using reverse transcription and a competitive polymerase chain reaction. *Journal of Pharmacology and Experimental Therapeutics* **275**, 1035–1042.
- SUN, X. D. & HERNES, S. (1996). Characterization of inwardly-rectifying potassium currents from dissociated rat taste receptor cells. *American Journal of Physiology* **271**, C1221–1232.
- TAKEDA, M. & KITAO, K. (1980). Effect of monoamines on the taste buds in the mouse. *Cell and Tissue Research* **210**, 71–78.
- TAKEDA, M., SHISHIDO, Y., KITAO, K. & SUZUKI, Y. (1982). Monoamines of taste buds in the fungiform and foliate papillae of the mouse. *Archivum Histologicum Japonicum* **45**, 239–246.
- TROISPOUX, C., REITER, E., COMBARNOUS, Y. & GUILLLOU, F. (1998). β 2 adrenergic receptors mediate cAMP, tissue-type plasminogen activator and transferrin production in rat Sertoli cells. *Molecular and Cellular Endocrinology* **142**, 75–86.
- VIDOVIC, M., COHEN, D. & HILL, C. E. (1994). Identification of α adrenergic receptor gene expression in sympathetic neurones using polymerase chain reaction and in situ hybridization. *Molecular Brain Research* **22**, 49–56.
- YAMAMOTO, T., NAGAI, T., SHIMURA, T. & YASOSHIMA, Y. (1998). Roles of chemical mediators in the taste system. *Japanese Journal of Pharmacology* **76**, 325–348.
- ZHAO, F. L., LU, S. G. & HERNES, S. (2002) Dual actions of caffeine on voltage-dependent currents and intracellular calcium in taste receptor cells. *American Journal of Physiology – Regulatory, Integrative and Comparative Physiology* **283**, R115–129.
- ZHAO, J., ARAKI, N. & NISHIMOTO, S. K. (1995). Quantitation of matrix Gla protein mRNA by competitive polymerase chain reaction using glyceraldehyde-3-phosphate dehydrogenase as an internal control. *Gene* **155**, 159–165.

Acknowledgement

This work was supported by grants NIH NIDCD DC00401 and NSF IBN 9724062.